View metadata, citation and similar papers at core.ac.uk

brought to you by CORE

provided by IUPUIScholarWorks

Article Type: Article

Accepted Article

Quantitative Prediction of CYP3A4 and CYP3A5-Mediated Drug Interactions

Yingying Guo[1*#], Aroonrut Lucksiri[2#], Gemma L. Dickinson[1], Raj K. Vuppalanchi[3], Janna K. Hilligoss[4], and Stephen D. Hall[1]

1. Drug Disposition, Eli Lilly and Company, Lilly Corporate Center, DC0714, Indianapolis, IN 46285, USA; guo_yingying@lilly.com, Tel: 317-277-4324; dickinson_gemma_louise@lilly.com; Tel: 317-433-1629; hall_stephen_d@lilly.com, Tel: 317-277-0338
2. Department of Pharmaceutical Care, Faculty of Pharmacy, Chiang Mai University, Chiang Mai, Thailand; noilucksiri@hotmail.com
3. Division of Gastroenterology and Hepatology, Indiana University School of Medicine, Indianapolis , IN 46202; rvuppala@iupui.edu; Tel: 317-944-0980
4. Department of Medicine, Indiana University, Indianapolis , IN 46202; jhilligo@iupui.edu

***Corresponding author**

Yingying Guo, PhD, Drug Disposition, Eli Lilly and Company, Lilly Corporate Center, DC0714, Indianapolis, IN 46285, USA; **Telephone:** (317) 277-4324, **E-mail:** guoying@lilly.com

# Both authors have made equal contribution to the manuscript

---

This is the author's manuscript of the article published in final edited form as:

Guo, Y., Lucksiri, A., Dickinson, G. L., Vuppalanchi, R. K., Hilligoss, J. K., & Hall, S. D. (n.d.). Quantitative Prediction of CYP3A4 and CYP3A5-Mediated Drug Interactions. Clinical Pharmacology & Therapeutics, 0(ja). https://doi.org/10.1002/cpt.1596

Accepted Article

Keywords: CYP3A4, CYP3A5, Physiologically-Based Pharmacokinetics, In Vitro, In-Vitro in-Vivo Correlation, Drug Development, Drug-Drug Interactions

Conflict of interest: Y.G., G.L.D., and S.D.H are employees and stockholders of Eli Lilly and Company. The contents of this article reflect the views of the authors and should not be construed to represent the views or policies of the FDA or the National Institutes of Health. No official support or endorsement by the FDA is intended or should be inferred. The mention of commercial products, their sources, or their use in connection with material reported herein is not to be construed as either an actual or implied endorsement of such products by the FDA.

Funding: This work was supported by NIH Grants T32GM08425, M01-RR00750, Food and Drug Administration Co-operative agreement FDT-001756, and a Royal Thai Scholarship.

Abbreviations:

CYP3A, cytochrome P450 3A; DDI, drug-drug interaction; AUCR, ratio of area under the curve; PBPK, physiologically-based pharmacokinetic; CL_{po}, oral clearance; CL_{sys}, systemic clearance; F_G, intestinal availability; CV, coefficient of variance; $f_{m,\ CYP3A5}$, fractional clearance of drugs by CYP3A5; $Ki_{,3A5}/Ki_{,3A4}$, ratio of reversible inhibitory potential towards CYP3A5 and CYP3A4; GCRC, Indiana University General Clinical Research Center.

This article is protected by copyright. All rights reserved.

Accepted Article

Abstract

We verified a physiologically-based pharmacokinetic (PBPK) model to predict cytochrome P450 3A4/5-mediated drug-drug interactions (DDIs). A midazolam-ketoconazole interaction study in 24 subjects selected by *CYP3A5* genotype, and LC/MS-quantification of CYP3A4/5 abundance from independently acquired and genotyped human liver (n=136) and small intestinal (N=12) samples were conducted. The observed *CYP3A5* genetic effect on midazolam systemic and oral clearance was successfully replicated by a mechanistic framework incorporating the proteomics-informed CYP3A abundance and optimized small intestinal CYP3A4 abundance based on midazolam intestinal availability (F_G) of 0.44. Furthermore, combined with a modified ketoconazole PBPK model, this framework recapitulated the observed geometric mean ratio of midazolam area under the curve (AUCR) following 200mg or 400mg ketoconazole, which was, respectively, 2.7-3.4 and 3.9-4.7 fold in intravenous administration, and 11.4-13.4 and 17.0-19.7 fold in oral administration, with AUCR numerically lower (P>0.05) in CYP3A5 expressers than non-expressers. In conclusion, the developed mechanistic framework supports dynamic prediction of CYP3A-mediated DDIs in study planning by bridging DDIs between CYP3A5 expressers and non-expressers.

Introduction

Cytochrome P450 3A4/5-mediated interactions continue to be commonly encountered as these enzymes are involved in the metabolic clearance and systemic bioavailability of more than half of the marketed drugs [1]. In adults, CYP3A4 and CYP3A5 are the most abundant CYPs in the human liver and small intestinal epithelium [2]. Oral clearance of CYP3A

This article is protected by copyright. All rights reserved.

substrates displays considerable inter-individual variability due to environmental, dietary, pathologic and genetic modulation of enzyme activity at both hepatic and intestinal sites [3]: *CYP3A4* genetic variation only explains approximately 5% of variability [4]. In contrast, genetic polymorphisms of *CYP3A5* significantly contribute to the inter-individual variability in metabolic clearance of some CYP3A-metabolized drugs [5]. *CYP3A5*3* is the most common non-functional *CYP3A5* allele [6] with differential distribution among ethnic groups [7]. CYP3A4 and CYP3A5 also share many common substrates, and the inhibition potency of many CYP3A inhibitors differ for CYP3A4 and CYP3A5 [8], further adding to the complexity of CYP3A-mediated DDIs.

Prediction of the magnitude of CYP3A-mediated DDIs is challenging. Physiologically-based pharmacokinetic (PBPK) modeling has not been successful in bringing together the relevant drug properties, physiological components including liver and gut CYP3A4/5, and the *CYP3A5* genetic polymorphism to predict CYP3A-mediated DDIs. One of the contributing factors is lack of characterization of gut CYP3A interactions and outcomes following perturbation of the system by inhibition. Furthermore, limited well-characterized data exists that adequately describes the expressions and relationships of gut CYP3A4 and CYP3A5.

We therefore had two objectives in the study. Our first objective is to deconvolute the complex interactions between liver and gut CYP3A4 and CYP3A5 using a clinical CYP3A-mediated DDI study with intravenous and oral administration of a CYP3A substrate in different *CYP3A5* genotypes. We hypothesized that for a CYP3A inhibitor that preferentially inhibits CYP3A4, magnitude of CYP3A inhibition may differ between CYP3A5 expressers, i.e. individuals carrying at least one *CYP3A5* functional allele (i.e. *1), and non-expressers, i.e.

Accepted Article

This article is protected by copyright. All rights reserved.

individuals who do not have functional CYP3A5. Ketoconazole was chosen as the clinical CYP3A inhibitor because it preferentially inhibits CYP3A4 [9] and has been commonly used to define CYP3A involvement in the systemic availability and/or clearance of a CYP3A substrate. Midazolam was selected as the CYP3A substrate as both CYP3A4 and CYP3A5 efficiently metabolize it *in vitro* [10]. Furthermore, its systemic clearance and oral bioavailability are commonly used to quantify clinical CYP3A activity because it displays substantial and selective metabolism by gut and liver CYP3A enzymes with minimal influence of drug transporters [11]. Our second aim is to exploit a PBPK modeling approach to predict CYP3A-mediated DDIs by integrating LC/MS measured CYP3A abundance and optimized small intestinal CYP3A4 abundance. We employ a single compartment first-order absorption model but recognize that a more complex segmented model of the gastro-intestinal tract will be necessary to recover drug-drug interactions for a drug that undergoes distal absorption [12]. Modeling not only helps understand and rationalize the clinical study results, but also allows prediction of situations where CYP3A5 genotypes may cause differences in CYP3A-mediated drug disposition and DDIs.

RESULTS

Clinical Midazolam- Ketoconazole Interaction Study

The serum concentration-time profiles of midazolam by *CYP3A5* genotypes following intravenous and oral doses are shown in Figure 1. Initial *CYP3A5*3* genotyping resulted in eight subjects in each of the *CYP3A5*1/*1*, *CYP3A5*1/*3* and *CYP3A5*3/*3* groups. Subsequent genotyping for *CYP3A5*6* and *CYP3A5*7* revealed *CYP3A5*1/*6* and *CYP3A5*3/*7*. The PK parameters of the five genotypes are presented in Table 1 with the

This article is protected by copyright. All rights reserved.

Accepted Article

*CYP3A5*3/*7* being considered individually as its phenotype cannot be unequivocally assigned [13]. The groups with ≥1 copy of the *CYP3A5*1* were combined into one CYP3A5 expresser group as they did not differ statistically significantly in C_{max} and clearance values. Compared to CYP3A5 non-expressers, oral clearances of midazolam (CL_{po}) were not significantly higher (geometric mean±SD) (140±66 vs 105±41 L/hr, *P*=0.13), but systemic clearances of midazolam (CL_{sys}) were significantly higher (32.8±7.95 vs 24.1±4.19 L/hr, *P*=0.002), and C_{max} values were significantly lower (1.6±0.6 vs 2.4±0.6, *P*=0.011) in CYP3A5 expressers. Hepatic extraction ratio in CYP3A5 expressers was approximately 30% higher than that of non-expressers (0.30±0.10 vs 0.22±0.04), but intestinal availability (F_G) in both groups was comparable (0.35±0.09 vs 0.33±0.06), suggesting lack of correlation between intestinal and hepatic availability of orally administered midazolam and differential regulation of hepatic and intestine CYP3A4, similar to other studies [11, 14].

As expected, ketoconazole 200 and 400 mg doses had a similar effect on midazolam C_{max} as both doses caused almost complete inhibition of gut CYP3A. The increase in midazolam AUC at the 400 mg ketoconazole dose was greater than that observed at the 200 mg dose but not proportional to the increase in ketoconazole exposure as the maximal inhibition of CYP3A in the liver is approached (Table 1). CL_{sys} values (geometric mean±SD) in CYP3A5 expressers and non-expressers were, respectively, 12.1±4.62 and 7.1± 2.0 L/hr after 200 mg, and 8.4±2.8 and 5.2±1.4 L/hr after 400 mg ketoconazole. CL_{po} values in CYP3A5 expressers and non-expressers were, respectively, 13.3± 5.6 and 7.0±2.0 L/hr after doses of 200 mg, and 8.4±3.5 and 4.9±1.3 L/hr after 400 mg ketoconazole. In other words, following 200mg or 400mg ketoconazole, the geometric mean ratio of the midazolam AUC (AUCR) was, respectively, 2.71-3.37 and 3.9-4.68 fold in intravenous administration, and 11.4-13.4 and

This article is protected by copyright. All rights reserved.
Accepted Article

17.0-19.7 fold in oral administration, but was not associated with *CYP3A5* genotype (Table S1). Additionally, there was no significant difference in the $AUC_{0\text{-}10hr}$ of ketoconazole 200 mg or 400 mg between the 6th and 7th day of dosing (Figure S1), nor significant differences in ketoconazole PK parameters among the groups with different copies of *CYP3A5*1* allele for any given ketoconazole dose (Table S2). Inclusion of the *CYP3A5*3/*7* individual in the group with 0 or 1 copy of *CYP3A5*1* did not influence any of these findings above (data not shown).

CYP3A Abundance and Midazolam Hydroxylation Activity

Proteomic analyses [15, 16] identified large variability in the CYP3A abundance within a group of genotyped human liver (N=136) and small intestinal (N=12) samples enriched for CYP3A5 expressers (Table 2). As *CYP3A5*1/*1* and *CYP3A5*1/*3* carriers did not differ in midazolam clearance (Table 1), both groups were also combined to increase sample size in analyzing CYP abundance. In CYP3A5 expressers, hepatic and small intestinal CYP3A5, but not CYP3A4 abundance ($P>0.05$), was significantly higher than those of non-expressers (Table 2). Within CYP3A5 expressers, significant correlation between CYP3A4 and CYP3A5 abundance was observed in liver (Fig. 2a, Rs 0.63, $P<0.05$) and small intestine (Fig. 2b, Rs 0.60, $P<0.05$). Additionally, for hepatic (Figure 2c) and small intestinal (Figure 2d) microsomal samples, there existed good correlation between total CYP3A abundance and activity that was determined by the formation of 1'-hydroxymidazolam at approximately the V_{max} range.

Accepted Article

This article is protected by copyright. All rights reserved.

The mean abundance ratio of small intestinal CYP3A4 and CYP3A5 was determined to be, respectively, 6.8 (12.3 to 1.81 pmol/mg) and 175.8 (12.3 to 0.07 pmol/mg) in CYP3A5 expressers and non-expressers (Table 2). The CYP3A4 abundance in a PBPK modelling software, SimCYP, was increased from 66.2 to 130 nmol/small intestine to reduce MDZ F_G from 0.56 to 0.44 [11] for CYP3A5 non-expressers. Subsequently the mean abundance ratios were used to adjust the CYP3A5 content in SimCYP from 24.6 and 0, respectively, to 19.1 and 1.13 nmol/small intestine for CYP3A5 expressers and non-expressers, respectively.

Simulation of *CYP3A5* Genetic Impact on Midazolam *in vivo* Clearance. The capability of PBPK models to reproduce midazolam blood clearance vs time profiles incorporating different hepatic and small intestinal CYP3A abundance in both CYP3A5 phenotypes were compared (Table 3 and Table S3). The proteomics-informed CYP3A abundance and variability that included 33% of measured coefficient of variance (CV) value from the human liver microsomal samples in conjunction with optimized small intestinal CYP3A abundance (scenario 5, Table S3) performed best and was utilized for subsequent simulations unless noted.

Simulation of *CYP3A5* Genetic Effects on Tacrolimus *in vivo* Clearance. *CYP3A5* genetic effects have been consistently demonstrated on tacrolimus clearance [5]. Using the proteomics-informed CYP3A abundance and variability, the modified tacrolimus SimCYP compound file (Table S4) adequately recovered the observed oral blood clearance in CYP3A5 expressers and non-expressers (Table S5a), and the PK in Caucasians and Africans (Figure S2 and Table S5b).

This article is protected by copyright. All rights reserved.

Accepted Article

Simulation of Midazolam-Ketoconazole Interactions. The modified ketoconazole model in SimCYP (Table S6) adequately recovered the serum PK of ketoconazole orally administered at 200mg and 400 mg (Figure S3a and S3b), but under-estimated those following 600 mg and 800 mg dose (data not shown). Among the 17 published midazolam- ketoconazole interaction studies with different study designs [17], 65% (11/17) of the study point estimates of AUCR, and 82% (14/17) of the 90% confidence interval were estimated within 1.5-fold of the observed (Figure S4).

Moreover, by integrating the proteomics-informed CYP3A abundance and variability, the modified ketoconazole model adequately recovered the inhibition of ketoconazole 200 mg and 400 mg QD towards midazolam PK and clearance in CYP3A5 expressers and non-expressers (Fig. 3a-f and Table S7). More importantly, the predicted AUCR of midazolam following ketoconazole is similar to the observed value, and slightly lower in the CYP3A5 expressers than non-expressers as observed.

Simulation of the Effects of CYP3A5 Metabolism and Differential Inhibition toward CYP3A5 and CYP3A4 on CYP3A-Mediated Drug Disposition and DDIs in CYP3A5 Expressers and Non-expressers. We formulated hypothetical studies focusing on how co-substrates of CYP3A4 and CYP3A5 would change in metabolic clearance and DDIs with two important variables: 1) relative contributions of CYP3A5 and CYP3A4 to substrate metabolism, and 2) differential inhibitory potential of a CYP3A inhibitor towards CYP3A5 and CYP3A4 (Ki ratio (CYP3A5/CYP3A4) or $Ki_{,3A5}/Ki_{,3A4}$) [18]. CYP3A5 genetic effects on the hypothetical CYP3A substrate, as shown by the clearance ratio of expressers to non-expressers, increased with increasing relative catalytic efficiency of CYP3A5 (Fig. 4a-4b and Table S8). CL_{sys} and CL_{po} of

This article is protected by copyright. All rights reserved.

CYP3A5 expressers ranged from 1.2- and 1.4- fold to 2.3- and 4-fold of non-expressers, respectively, when the relative contribution of CYP3A5 to metabolism ranges from equal to 9 times that of CYP3A4.

Following treatment with the hypothetical CYP3A inhibitor, the CL_{sys} and CL_{po} of a CYP3A substrate remained higher in CYP3A5 expressers than non-expressers (data not shown). Within a given administration route of the substrate, the magnitude of inhibition within the CYP3A5 expressers increased with increasing inhibitory potency toward CYP3A5 (Fig. 4c-4d and Table S8). Interestingly, the relative differences of AUCR between CYP3A5 expressers and non-expressers varied with the relative CYP3A5 metabolic contribution and the ratio of Ki toward CYP3A5 and CYP3A4. The higher the relative CYP3A5 contribution, the higher the $Ki,_{3A5}/Ki,_{3A4}$ that would need to achieve a comparable or higher AUCR in CYP3A5 expressers compared to non-expressers.

DISCUSSION

In the present study, we have described a clinical CYP3A-mediated DDI study to inform a PBPK framework that successfully recapitulated midazolam and ketoconazole interactions in the absence and presence of CYP3A5 expression. The framework builds upon optimized small intestinal CYP3A4 abundance and integrates the proteomics-informed CYP3A abundance from genotyped human liver (n=136) and small intestinal (N=12) samples. The PBPK model was also qualified by recovering the significant *CYP3A5* genetic effects on tacrolimus disposition. Hypothetical DDI studies were subsequently simulated to demonstrate utility of the framework in predicting CYP3A5 contribution to CYP3A-mediated disposition and DDIs.

Accepted Article

This article is protected by copyright. All rights reserved.

The clinical DDI study was consistent with literature on the overall understanding of ketoconazole inhibition and *CYP3A5* genetic effects. First, ketoconazole increased midazolam exposure in a dose-dependent manner and also at a magnitude within the ranges of the 17 published ketoconazole-midazolam studies [17]. Second, consistent with previous findings [5, 19-22], an overall weak influence of *CYP3A5* genetics on midazolam metabolism was observed. In this study, CYP3A5 expressers had approximately 30% higher CL_{sys} and CL_{po} relative to non-expressers. But due to the markedly lower inter-individual variability for the CL_{sys} (2.3-fold), comparing to that of CL_{po} (7.0-fold) and other studies (3.3- to 5.2-fold) [21-24], only the CL_{sys} change reached statistical ($p<0.05$, Table 1) with unlikely clinical significance. Third, *CYP3A5* genotype appeared to have no significant effect on the midazolam AUCR upon ketoconazole treatment, with AUCR only slightly lower ($P>0.05$) in CYP3A5 expressers than non-expressers (Table 1). Although somewhat surprising, this is in agreement with the data of Halama et al. that evaluated the interactions of ketoconazole 400 mg QD with orally administered midazolam [25]. Another potent CYP3A5 competitive inhibitor fluconazole also did not result in differential changes of midazolam metabolites formation across CYP3A5 genotypes [26].

Importantly, the clinical DDI study allowed a deconvolution of the contribution of CYP3A4 and CYP3A5 towards first-pass hepatic and gut metabolism, which was critical in qualifying our F_G optimization approach. Systemic clearance and AUCR from the midazolam intravenous administration in the CYP3A5 non-expressers before and after ketoconazole treatments informed estimation of first-pass hepatic CYP3A4 contribution (Table 1). Combined with the dataset from the midazolam oral administration, the first-pass gut

This article is protected by copyright. All rights reserved.

Accepted Article

CYP3A4 contribution was delineated (Table 1). In SimCYP, midazolam F_G (0.57) was derived using plasma clearance and hepatic plasma flow, assuming midazolam partition into red blood cells was negligible [27]. This is not necessarily a valid assumption given the midazolam blood to serum concentration ratio was 0.56-0.66 at the serum concentration of 10-150 ng/ml [11]. We aimed to adjust midazolam F_G to approximately 0.44 that was obtained using blood clearance and hepatic blood flow [11]. Midazolam F_G in SimCYP is calculated using a Q_{gut} model basing on a nonlinear relationship of gut intrinsic clearance and gut blood flow. As we cannot directly input our small intestinal microsomal CYP3A4 abundance data into SimCYP due to lack of the data collection parameters needed for conversion [28], we optimized it in SimCYP from 66.2 to 130 nmol/small intestine leading to midazolam F_G of 0.44 in CYP3A5 non-expressers. This approach drastically improved magnitude of CYP3A4-mediated DDI by adequately recovering the first-pass gut CYP3A4 contribution (Fig. 3 and Table S7). By contrast, without such optimization, midazolam AUCR was markedly under-estimated regardless of ketoconazole model and hepatic CYP3A abundance (Table S9). It should be noted that this optimization of abundance was in the context of the single absorption compartment with a first-order model and should be revisited if other absorption models are employed.

The proteomics-informed CYP3A abundance has improved the mechanistic framework of CYP3A-mediated DDI prediction. The LC/MS-measured hepatic CYP3A4 content reasonably recovered midazolam CL_{sys} in CYP3A5 non-expressers (Table 3&4). Furthermore, the dataset was consistent with the literature: 1) good correlation between the CYP3A abundance and activity (Figure 2c and 2d); 2) previous literature [29] supports the finding that the mean

This article is protected by copyright. All rights reserved.

hepatic and small intestinal CYP3A4 abundance did not significantly differ between CYP3A5 expressers and non-expressers (Table 2); 3) the mean hepatic CYP3A4 and CYP3A5 abundance (Table 2) was consistent with that from a meta-analysis of 50 studies [30]. Additionally, as artificial variability exists in human liver banks due to sources, procurement, processing, and treatment, hepatic CYP3A4 and CYP3A5 variabilities were reduced from 98% and 92% to 32% and 30%, respectively, to improve prediction of variability for CYP3A4 substrates, similar to previous approaches [31]. The optimized CYP3A4 abundance variability of 32% is similar to 33% that was used to simulate the reported CV values of AUC for multiple CYP3A4 substrates [32].

The proteomic dataset has re-defined relationships of CYP3A4 and CYP3A5 in liver and gut, which were further qualified in the study. Comparing to the SimCYP values [33], our dataset trended lower in hepatic CYP3A4 and CYP3A5 abundance (80.1 and 23.8 versus 137 and 103 pmol/mg, respectively), and in the CYP3A4 vs CYP3A5 correlation (correlation coefficient 0.18 versus 0.38) (Table S2). Additionally, for the first time, the ratios of small intestinal CYP3A4 to CYP3A5 abundance in different CYP3A5 phenotypes were characterized (Table 2), enabling estimation of the small intestinal CYP3A5 abundance based on the optimized CYP3A4 content in SimCYP (Table S2). The re-defined relationships of CYP3A4 and CYP3A5 in liver and gut well recovered *CYP3A5* genetic effects on IV and oral clearance of midazolam and tacrolimus (Table 3, Table S5 & Figure S2). Furthermore, they enabled recapitulating the slightly lowered midazolam AUCR in the CYP3A5 expressers than non-expressers following ketoconazole treatment (Fig. 3). The Ki values of ketoconazole towards CYP3A4 and CYP3A5 are 0.01 μM (5 ng/mL) and 0.109 μM (58 ng/mL), respectively, when midazolam is the

This article is protected by copyright. All rights reserved.

CYP3A probe [9]. Under the simulated ketoconazole concentrations in liver and small intestine, CYP3A4 activity was inhibited to a larger extent than CYP3A5 as demonstrated by the higher hepatic and small intestinal intrinsic clearance in CYP3A5 expressers than non-expressers (Figure S5a-S5b). As a result of interplays among uninhibited CYP3A5 protein, CYP3A5 metabolic activity, and reduction of CYP3A4 activity ascribed to CYP3A4 inhibition, midazolam AUCR in CYP3A5 expressers turned out to be only slightly lower than non-expressers following ketoconazole treatment. The utility of the proteomics-informed CYP3A abundance and variability in simulating and modeling other CYP3A substrate(s) in SimCYP settings warrants further follow up.

Previously, a ketoconazole PBPK model that incorporated a saturable efflux process in the liver compartment has improved the prediction of CYP3A inhibition [17, 34]. We have translated the approach into SimCYP by engineering uptake and efflux transporter-like mechanisms in the liver (Table S6). The modified model was demonstrated to describe the nonlinear ketoconazole accumulation at the enzyme site in a dose-dependent manner (Figure S5c-S5d), leading to higher extent of hepatic and intestinal CYP3A inhibition in the 400mg relative to the 200mg ketoconazole treatment. The modified model recapitulated the inhibition of 200mg and 400 mg ketoconazole QD towards midazolam PK and clearance in CYP3A5 expressers and non-expressers (Fig. 3). By contrast, the SimCYP ketoconazole 400 mg QD model (v.17R1) would markedly under-estimate such interactions (Table S9). The modified ketoconazole model is a practical solution to predict the worst-case scenario of CYP3A-mediated inhibition within SimCYP.

This article is protected by copyright. All rights reserved.

Accepted Article

The mechanistic framework qualified here also illustrated the importance of determining if an investigational drug is a substrate and/or inhibitor of CYP3A5 in addition to CYP3A4 and has enabled us to predict the impact of CYP3A5 expression on the pharmacokinetics and DDIs of CYP3A substrates. First, fractional clearance of drugs by CYP3A5 ($f_{m, CYP3A5}$) must be at least 0.34 (total hepatic CL_{int} 1234 L/h) for *CYP3A5* genetics to become a major contributor to total intrinsic clearance (Fig. 4a-4b). In addition, both the $f_{m, CYP3A5}$ and the Ki ratio (CYP3A5/CYP3A4) ($Ki,_{3A5}/Ki,_{3A4}$) should be considered when predicting impact of CYP3A5 expression on a strong CYP3A inhibitor mediated DDIs: 1) If $f_{m, CYP3A5} \leq 0.34$ and $Ki,_{3A5}/Ki,_{3A4} \geq 7$, CYP3A5 non-expressers would have comparable or higher oral AUCR than expressers; 2) If $f_{m, CYP3A5} \geq 0.22$ and $Ki,_{3A5}/Ki,_{3A4} < 7$, CYP3A5 expressers would have higher oral AUCR than non-expressers and CYP3A5 is important for accurate predictions; and 3) If $f_{m, CYP3A5} < 0.22$ but $Ki,_{3A5}/Ki,_{3A4} < 7$, or $f_{m, CYP3A5} > 0.34$ but $Ki,_{3A5}/Ki,_{3A4} > 7$, the modeling framework should be used to predict the AUCR in different CYP3A5 phenotypes to support subject selection in study design and prioritization by bridging DDIs between the two groups.

Such a roadmap has important clinical implications. First, it helps set up criteria of initiating *CYP3A5* genotyping and aids power analyses in designing *CYP3A5* genetic studies by quantitatively predicting *CYP3A5* genetic influence on PK. Second, it applies to designing and conducting index or concomitant DDI studies for CYP3A substrates. Itraconazole is a FDA-recommended index CYP3A inhibitor that preferentially inhibits CYP3A4 or $Ki,_{3A5}/Ki,_{3A4} \geq 7$ [18]. It is predicted that the magnitude of itraconazole interaction with a co-substrate of CYP3A4 and CYP3A5 with $f_{m, CYP3A5} \leq 0.34$, such as midazolam, would be lower in CYP3A5 expressers (Fig. 4 and Table S8), in agreement with a previous report [21]. Consequently, it may become a concern in ethnic groups with higher percentage of CYP3A5

This article is protected by copyright. All rights reserved.

Accepted Article

expressers such as Africans and Asians [7] that the worst-case scenario of CYP3A inhibition may not be revealed. Additional clinical CYP3A-mediated DDI studies in CYP3A5-genotyped populations for CYP3A drugs $f_{m, CYP3A5} \geq 0.34$, i.e. tacrolimus and vincristine[35], may be warranted to advance understanding of role of CYP3A5 inhibition/content in adequate DDI predictions. Another scenario is when conducting concomitant DDI studies using a co-substrate of CYP3A4 and CYP3A5, such as simvastatin with equal CYP3A4 and CYP3A5 contribution ($f_{m, CYP3A5} \geq 0.22$) [36]. When $Ki_{,3A5}/Ki_{,3A4}$ is lower than five, the AUCR is predicted to be markedly higher in CYP3A5 expressers than that in non-expressers (Fig. 4 and Table S8), and then DDIs from a study with primarily CYP3A5 non-expressers may not reflect those in expressers. Although this scenario remains to be clinically validated, it deserves much attention considering the wide use of simvastatin in the polypharmacy era, less-well-understood CYP3A5 inhibition by known CYP3A4 inhibitors[37], as well as emerging compounds with potent CYP3A5 reversible inhibition ($Ki_{,3A5}/Ki_{,3A4} \leq 1$) in drug development.

In conclusion, aided by a clinical CYP3A-mediated DDI study of oral and intravenous administration of midazolam with ketoconazole in different CYP3A5 genotypes, a PBPK framework incorporating proteomics-informed hepatic and small intestinal CYP3A abundance in combination with optimized small intestinal CYP3A4 content was qualified in SimCYP and used to predict CYP3A-mediated DDIs. The modeling suggested the importance of evaluating the potential of an investigational drug to be a substrate and inhibitor of CYP3A5. The PBPK modeling framework may be applied to PK and DDI studies of CYP3A substrate(s) in supporting study design and prioritization by bridging DDIs between CYP3A5 expressers and non-expressers.

This article is protected by copyright. All rights reserved.

Accepted Article

Methods

Clinical Study

Subjects. This study was approved by the Clarian and Indiana University Purdue University at Indianapolis institutional review board and the Research Involving Human Subjects Committee (FDA, DHSS). Twenty-four volunteers participated in the study after giving written informed consent. This 3-phase partially randomized cross-over study was conducted at the Indiana University General Clinical Research Center (GCRC). There was a washout period of at least 7 days but no longer than 14 days between the two adjacent study phases. All subjects were 18 years or older healthy subjects with inclusion criteria and clinical CYP3A5 genotyping methods were detailed in Supplementary Methods.

Study Phase 1 (Control Phase). After an overnight fast, the volunteers received a 0.05 mg/kg dose of midazolam (Versed®) infused intravenously over 30 minutes into an antecubital vein under the supervision of a physician. Blood samples (5 ml) were collected from an indwelling venous catheter at the 0.5, 0.75, 1, 1.5, 2, 4, 6, 9, and 24 hours following the start of the infusion. Subjects were allowed to eat 4 hours post dosing. Immediately after the 24 hr blood collections, an oral dose of midazolam 4 mg (Roxane Laboratory, Inc., Columbus, OH) was administered with 240 ml of water, and blood samples were collected as described above.

Study Phase 2 and 3 (First and Second Ketoconazole Dosing). The volunteers were randomized to receive ketoconazole 200 mg or 400 mg (Taro Pharmaceutical Industries Ltd, Hawthorne, NY) each morning with a can of caffeine-free cola (Coca-cola Company, Atlanta, Georgia) for 7-days. On the sixth day of ketoconazole dosing, subjects returned to the GCRC and one hour after the ketoconazole, a 0.0125 mg/kg dose of midazolam was infused

This article is protected by copyright. All rights reserved.

intravenously over 30 minutes and blood samples (7 mL) obtained as described in Phase 1. On the seventh day of ketoconazole, one hour after ketoconazole and 24 hours after midazolam administration on the previous day, a 1 mg of midazolam was orally administered and blood samples (7 mL) were collected as described in Phase 1. The volunteers initiated the second ketoconazole regimen (200 mg or 400 mg) and underwent the same dosing and blood sampling as Phase 2. Serum samples were stored at -20°C until analysis. Serum concentrations of ketoconazole, midazolam and 1'-hydroxymidazolam were quantified by LC-MS as described previously [38, 39]. All data analysis were conducted and detailed in Supplementary Methods.

In Vitro Studies

Human Liver and Small Intestinal Samples. A total of 136 human liver samples and 12 human intestinal samples were utilized. Among them, 121 human liver microsomes (HLMs) were isolated from human liver tissues as previously described [40] and the sample sources and demographics are provided in Table S10. Additional 15 HLMs from donors previously confirmed for *CYP3A5* genotypes were obtained from vendors. The 12 human intestinal microsomes (HIMs) were acquired from Bioreclamation IVT (Baltimore, MD).

LC/MS Quantification of CYP3A Abundance. A stable isotope labeling (SIL)-based targeted quantitative proteomic approach was used to quantify CYP3A4 and CYP3A5 abundance in the 136 HLMs as previously described [15]. A similar approach was used to measure CYP3A4 and CYP3A5 abundance in the 12 HIMs as previously detailed [16], with the exception that

This article is protected by copyright. All rights reserved.

Accepted Article

peptides (L_{477}SLGGLLQPEKPVVL**K**$_{492}$ and D_{244}TINFLS**K**$_{251}$) were used to quantify CYP3A4 and CYP3A5, respectively (personal communication with Dr. Phil Smith).

***In vitro CYP3A Midazolam Activity Assay*.** CYP3A activity as measured by the formation of 1'-hydroxymidazolam as a function of both the incubation time and protein concentration measured by BCA method, was quantified at a single substrate concentration of midazolam in 136 HLMs and 12 HIMs. Details on the HLM and HIM samples, *CYP3A5* genotyping, and *in vitro* CYP3A midazolam activity assay were described in Supplementary Methods.

Modeling and Simulation. Modeling and simulations were performed in the SimCYP Population-Based PBPK Simulator® (version 17R1, Certara, Princeton, NJ) to 1) simulate *CYP3A5* genetic impact on midazolam and tacrolimus *in vivo* clearance to verify use of LC/MS-measured CYP3A abundance, 2) qualify the modified ketoconazole model in SimCYP and then simulate midazolam-ketoconazole interactions, and 3) predict impact of CYP3A5 expression on CYP3A-mediated disposition and DDIs in hypothetical studies. The single absorption compartment first-order model was considered appropriate to reflect the absorption of substrates in immediate release formulations that have sufficient solubility and permeability to be absorbed in the small intestine where CYP3A enzymes are expressed [12]. Details on compound profile parameter settings, and the study design including study populations, drug administration, time course, and sampling are described in Supplementary Methods.

Accepted Article

This article is protected by copyright. All rights reserved.

Accepted Article

Study Highlights

What is the current knowledge on the topic?

CYP3A4/5-mediated interactions are commonly encountered but challenging to predict due to the associated complexity. CYP3A4 and CYP3A5 share many common substrates, and the inhibition potency of many CYP3A inhibitors differ for CYP3A4 and CYP3A5.

What question did this study address?

Can we improve CYP3A4/5-mediated DDIs by verifying a PBPK model that brings together the relevant drug properties, physiological components including liver and gut CYP3A4/5, and *CYP3A5* genetic polymorphisms?

What does this study add to our knowledge?

The presented PBPK modeling approach enables a better understanding of contribution of hepatic and small intestinal CYP3A4/5 abundance to the drug disposition and DDIs of CYP3A substrates. Scenarios where *CYP3A5* genotypes may significantly impact CYP3A-mediated DDIs are better understood and predicted.

How might this change clinical pharmacology or translational science?

A PBPK modeling framework incorporating proteomics-informed hepatic and small intestinal CYP3A abundance in combination with optimized small intestinal CYP3A4 content improves CYP3A-mediated DDI prediction. For PK and DDI studies of CYP3A substrate(s), such a framework can inform study design and prioritization by bridging DDIs between CYP3A5 expressers and non-expressers.

This article is protected by copyright. All rights reserved.

Accepted Article

Acknowledgments

The authors thank Steve Wrighton and Barbara Ring for their long-term efforts to establish this human liver tissue bank. The authors also thank Michael Mohutsky, Jiaqi Bao and Jessica Baker in Eli Lilly and Company for the valuable help with characterization of the human liver and intestinal samples; Mitchell A Hamman at the Indiana University School of Medicine for conducting the plasma sample bioanalysis; Scott Heyward in the Bioreclamation IVT for providing genotyped human intestinal samples that were critical for this study; and Michael Wang at the University of Kansas and Philip Smith at the University of North Carolina at Chapel Hill for their proteomic analyses of microsomal samples.

Author Contributions

Y.G., A.L., G.L.D., and S.D.H. wrote the manuscript; Y.G., A.L., G.L.D., R.K.V., J.K.H., and S.D.H. designed the research; Y.G. and A.L. performed the research; Y.G., A.L., G.L.D., and S.D.H. analyzed the data.

This article is protected by copyright. All rights reserved.

REFERENCES

1. Williams, J.A., et al., *Drug-drug interactions for UDP-glucuronosyltransferase substrates: a pharmacokinetic explanation for typically observed low exposure (AUCi/AUC) ratios.* Drug Metabolism and Disposition: The Biological Fate of Chemicals, 2004. **32**: p. 1201-1208.
2. Paine, M.F., et al., *The human intestinal cytochrome P450 "pie".* Drug Metab Dispos, 2006. **34**(5): p. 880-6.
3. Hohmann, N., W.E. Haefeli, and G. Mikus, *CYP3A activity: towards dose adaptation to the individual.* Expert Opin Drug Metab Toxicol, 2016. **12**(5): p. 479-97.
4. Werk, A.N. and I. Cascorbi, *Functional gene variants of CYP3A4.* Clin Pharmacol Ther, 2014. **96**(3): p. 340-8.
5. Tornio, A. and J.T. Backman, *Cytochrome P450 in Pharmacogenetics: An Update.* Adv Pharmacol, 2018. **83**: p. 3-32.
6. Kuehl, P., et al., *Sequence diversity in CYP3A promoters and characterization of the genetic basis of polymorphic CYP3A5 expression.* Nat Genet, 2001. **27**(4): p. 383-91.
7. Guo, Y., et al., *Deciphering ADME genetic data using an automated haplotype approach.* Pharmacogenet Genomics, 2014. **24**(6): p. 292-305.
8. Niwa, T., et al., *Comparison of kinetic parameters for drug oxidation rates and substrate inhibition potential mediated by cytochrome P450 3A4 and 3A5.* Curr Drug Metab, 2008. **9**(1): p. 20-33.
9. Gibbs, M.A., et al., *Inhibition of cytochrome P-450 3A (CYP3A) in human intestinal and liver microsomes: comparison of Ki values and impact of CYP3A5 expression.* Drug Metab Dispos, 1999. **27**(2): p. 180-7.
10. Gorski, J.C., et al., *Regioselective biotransformation of midazolam by members of the human cytochrome P450 3A (CYP3A) subfamily.* Biochem Pharmacol, 1994. **47**(9): p. 1643-53.
11. Gorski, J.C., et al., *The contribution of intestinal and hepatic CYP3A to the interaction between midazolam and clarithromycin.* Clin Pharmacol Ther, 1998. **64**(2): p. 133-43.

Accepted Article

This article is protected by copyright. All rights reserved.

Accepted Article

12. Olivares-Morales, A., et al., *Analysis of the impact of controlled release formulations on oral drug absorption, gut wall metabolism and relative bioavailability of CYP3A substrates using a physiologically-based pharmacokinetic model.* Eur J Pharm Sci, 2015. **67**: p. 32-44.
13. Hustert, E., et al., *The genetic determinants of the CYP3A5 polymorphism.* Pharmacogenetics, 2001. **11**(9): p. 773-9.
14. Tsunoda, S.M., et al., *Differentiation of intestinal and hepatic cytochrome P450 3A activity with use of midazolam as an in vivo probe: effect of ketoconazole.* Clin Pharmacol Ther, 1999. **66**(5): p. 461-71.
15. Wang, M.Z., et al., *A gel-free MS-based quantitative proteomic approach accurately measures cytochrome P450 protein concentrations in human liver microsomes.* Proteomics, 2008. **8**(20): p. 4186-96.
16. Fallon, J.K., et al., *Targeted quantitative proteomics for the analysis of 14 UGT1As and -2Bs in human liver using NanoUPLC-MS/MS with selected reaction monitoring.* J Proteome Res, 2013. **12**(10): p. 4402-13.
17. Han, B., et al., *Optimization of drug-drug interaction study design: comparison of minimal physiologically based pharmacokinetic models on prediction of CYP3A inhibition by ketoconazole.* Drug Metab Dispos, 2013. **41**(7): p. 1329-38.
18. Shirasaka, Y., et al., *Effect of CYP3A5 expression on the inhibition of CYP3A-catalyzed drug metabolism: impact on modeling CYP3A-mediated drug-drug interactions.* Drug Metab Dispos, 2013. **41**(8): p. 1566-74.
19. Miao, J., et al., *Association of genotypes of the CYP3A cluster with midazolam disposition in vivo.* Pharmacogenomics J, 2009. **9**(5): p. 319-26.
20. Kharasch, E.D., et al., *Influence of CYP3A5 genotype on the pharmacokinetics and pharmacodynamics of the cytochrome P4503A probes alfentanil and midazolam.* Clin Pharmacol Ther, 2007. **82**(4): p. 410-26.

This article is protected by copyright. All rights reserved.

21. Yu, K.S., et al., *Effect of the CYP3A5 genotype on the pharmacokinetics of intravenous midazolam during inhibited and induced metabolic states.* Clin Pharmacol Ther, 2004. **76**(2): p. 104-12.

22. Shih, P.S. and J.D. Huang, *Pharmacokinetics of midazolam and 1'-hydroxymidazolam in Chinese with different CYP3A5 genotypes.* Drug Metab Dispos, 2002. **30**(12): p. 1491-6.

23. Eap, C.B., et al., *Pharmacokinetics of midazolam in CYP3A4- and CYP3A5-genotyped subjects.* Eur J Clin Pharmacol, 2004. **60**(4): p. 231-6.

24. Floyd, M.D., et al., *Genotype-phenotype associations for common CYP3A4 and CYP3A5 variants in the basal and induced metabolism of midazolam in European- and African-American men and women.* Pharmacogenetics, 2003. **13**(10): p. 595-606.

25. Halama, B., et al., *A nanogram dose of the CYP3A probe substrate midazolam to evaluate drug interactions.* Clin Pharmacol Ther, 2013. **93**(6): p. 564-71.

26. Yang, J., et al., *Evidence of CYP3A allosterism in vivo: analysis of interaction between fluconazole and midazolam.* Clin Pharmacol Ther, 2012. **91**(3): p. 442-9.

27. Thummel, K.E., et al., *Oral first-pass elimination of midazolam involves both gastrointestinal and hepatic CYP3A-mediated metabolism.* Clin Pharmacol Ther, 1996. **59**(5): p. 491-502.

28. Paine, M.F., et al., *Characterization of interintestinal and intraintestinal variations in human CYP3A-dependent metabolism.* J Pharmacol Exp Ther, 1997. **283**(3): p. 1552-62.

29. Lin, Y.S., et al., *Co-regulation of CYP3A4 and CYP3A5 and contribution to hepatic and intestinal midazolam metabolism.* Mol Pharmacol, 2002. **62**(1): p. 162-72.

30. Achour, B., J. Barber, and A. Rostami-Hodjegan, *Expression of Hepatic Drug-Metabolizing Cytochrome P450 Enzymes and Their Inter-Correlations: A Meta-Analysis.* Drug Metab Dispos, 2014.

31. Cubitt, H.E., et al., *Sources of interindividual variability in IVIVE of clearance: an investigation into the prediction of benzodiazepine clearance using a mechanistic population-based pharmacokinetic model.* Xenobiotica, 2011. **41**(8): p. 623-38.

This article is protected by copyright. All rights reserved.

Accepted Article

Accepted Article

32. Kato, M., et al., *Prediction of interindividual variability in pharmacokinetics for CYP3A4 substrates in humans.* Drug Metab Pharmacokinet, 2010. **25**(4): p. 367-78.

33. Barter, Z.E., et al., *Determination of a quantitative relationship between hepatic CYP3A5*1/*3 and CYP3A4 expression for use in the prediction of metabolic clearance in virtual populations.* Biopharm Drug Dispos, 2010. **31**(8-9): p. 516-32.

34. Chien, J.Y., et al., *Stochastic prediction of CYP3A-mediated inhibition of midazolam clearance by ketoconazole.* Drug Metab Dispos, 2006. **34**(7): p. 1208-19.

35. Dennison, J.B., et al., *Selective metabolism of vincristine in vitro by CYP3A5.* Drug Metab Dispos, 2006. **34**(8): p. 1317-27.

36. Kim, K.A., et al., *Effect of polymorphic CYP3A5 genotype on the single-dose simvastatin pharmacokinetics in healthy subjects.* J Clin Pharmacol, 2007. **47**(1): p. 87-93.

37. Ragia, G., M.L. Dahl, and V.G. Manolopoulos, *Influence of CYP3A5 polymorphism on the pharmacokinetics of psychiatric drugs.* Curr Drug Metab, 2016. **17**(3): p. 227-36.

38. Wang, Z., et al., *The effects of St John's wort (Hypericum perforatum) on human cytochrome P450 activity.* Clin Pharmacol Ther, 2001. **70**(4): p. 317-26.

39. Belle, D.J., et al., *The effects of an oral contraceptive containing ethinyloestradiol and norgestrel on CYP3A activity.* Br J Clin Pharmacol, 2002. **53**(1): p. 67-74.

40. Steere, B., et al., *Prediction of in vivo clearance and associated variability of CYP2C19 substrates by genotypes in populations utilizing a pharmacogenetics-based mechanistic model.* Drug Metab Dispos, 2015. **43**(6): p. 870-83.

This article is protected by copyright. All rights reserved.

Accepted Article

Figure Legends

Figure 1. Serum (mean± SE) concentration-time profiles of midazolam via intravenous (a-c) and oral (d-f) administration in the absence (a and d, phase 1) and presence of 200 mg (b and e) or 400 mg (c and f) doses of ketoconazole (phase 2 and 3). CYP3A5 expressers are presented in solid lines and CYP3A5 non-expressers are presented in dotted lines.

Figure 2. Relationships between CYP3A4 abundance, CYP3A5 abundance and CYP3A metabolic activity in human liver and small intestinal microsomal samples. The correlation is shown between LC/MS-measured hepatic (a) and small intestinal (b) microsomal CYP3A4 and CYP3A5 content in the CYP3A5 expressers, respectively, from the human liver samples (*CYP3A5*1/*1*: N=11, and *CYP3A5*1/*3* or *CYP3A5*1/*6*: N=23) and small intestinal samples (*CYP3A5*1/*1*: N=2, and *CYP3A5*1/*3:* N=4). Correlation of total CYP3A content with the CYP3A activity as measured by the formation rate of 1'-hydroxymidazolam is shown for the human hepatic (c) and small intestinal (d) microsomal samples. Among the total 136 liver tissues, 121 of them had microsomal samples for 1'-hydroxymidazolam formation assay, in which three *CYP3A5*1/*1*, one *CYP3A5*1/*3*, and 10 *CYP3A5*3/*3* samples didn't have activity data. Within the 12 small intestinal samples, one *CYP3A5*1/*3* and two *CYP3A5*3/*3* samples had activity data below the lower limit of quantification and were excluded from analyses, which led to nine samples that were used for the activity and CYP3A content correlation analyses.

This article is protected by copyright. All rights reserved.

Accepted Article

Figure 3. Observed and simulated intravenous (IV) and oral pharmacokinetic parameters (geometric mean) of midazolam following oral administration of 200 mg or 400 mg ketoconazole (KTZ) in CYP3A5 non-expressers (non-exp) and expressers (exp). (a-c) The white and black bars represent, respectively, the observed and simulated midazolam IV blood clearance (a), oral blood clearance (b), and oral C_{max} (maximum blood concentration) normalized by dose (c) following KTZ treatments. (d-f) The white and black bars represent, respectively, the observed and simulated midazolam IV AUC ratio (d), oral AUC ratio (e), and C_{max}/dose ratio (f) following KTZ treatments. See Table S7 online more details.

Figure 4. Simulated interaction trials (geometric mean) of hypothetical CYP3A substrates (with different V_{max} ratio (CYP3A5/CYP3A4)) and hypothetical CYP3A inhibitors (with different Ki ratio (CYP3A5/CYP3A4)). Hypothetical substrates differed from midazolam in ADME properties only in the relative contribution of hepatic CYP3A5 and CYP3A4 to metabolism, ranging from equal contribution to nine times of contribution from CYP3A5. This was reflected by changing the ratio of Vmax value of 1'-hydroxymidazolam formation by CYP3A5 to CYP3A4 from 2 to 18 while maintaining a constant value for the overall intrinsic clearance of CYP3A-mediated 1'-hydroxymidazolam formation. Hypothetical CYP3A inhibitors differed from ketoconazole only in the Ki ratio for CYP3A5 and CYP3A4, ranging from 1 to 7 while keeping the CYP3A4 Ki as 0.01 µM. With the CL_{int} ratio of CYP3A5 to CYP3A4 is 1, 2, 4, and 9, the hepatic clearance of CYP3A5 expressers is 1484, 1234, 1019, and 876 L/h, and fractional clearance of drugs by CYP3A5 ($f_{m,CYP3A5}$) is 0.22, 0.34, 0.49 and 0.65, respectively. (a-b) The white and black bars represent the simulated IV (a) and oral (b) clearance values of the hypothetical substrate in, respectively, CYP3A5 non-expressers and

This article is protected by copyright. All rights reserved.

expressers following KTZ treatments. The numbers labelled on the top of black bars indicate the fold change in clearance values of CYP3A5 expressers relative to non-expressers. (c-d) The white bars represent the AUC ratio in CYP3A5 non-expressers with and without an inhibitor of $K_{i,CYP3A4}$ of 0.01 µM. Other symbols represent the AUC ratios in CYP3A5 expressers with and without an inhibitor of $K_{i,CYP3A4}$ of 0.01 µM but different Ki ratio (CYP3A5/CYP3A4): 7 (black), 5 (light vertical), 2 (downward diagonal), and 1(upward diagonal).

Supplementary Information Title

(Supplemental Materials.pdf)

Supplementary Materials: Supplementary Methods, Figures S1-S5, Table S1-10

Accepted Article

This article is protected by copyright. All rights reserved.

Accepted Article

Table 1. Disposition of midazolam alone and following 200 mg or 400 mg doses of ketoconazole (KTZ) stratified by CYP3A5 genotypes

	Control					*200 mg KTZ*					*400 mg KTZ*				
CYP3A5	*1/*1	*1/*3 and *1/*6	**Expressers**	*3/*3	*3/*7	*1/*1	*1/*3 and *1/*6	**Expressers**	*3/*3	*3/*7	*1/*1	*1/*3 and *1/*6	**Expressers**	*3/*3	*3/*7
	(n=6)	(n=9)	**(n=15)**	(n=8)	(n=1)										
Cmax /Dose (ng/mL)	1.5 (24)	1.6 (49)	**1.6 (40)**	2.4 (27)	3.4	9.6 (42)	7.9 (47)	**8.5 (44)**	12.3 (26)	18.1	9.4 (44)	8.9 (44)	**9.1 (42)**	15.8 (21)	21.2
p-value#			**0.011**		n/a			**0.021**		n/a			**0.0004**		n/a
Tmax (hr)*	0.75 (0.5-1)	0.75 (0.5-1)	**0.7**	0.76 (0.5-1.5)	1	0.75 (0.5-1.5)	1 (0.5-1)	**0.8**	1.5 (0.5-2)	1.5	0.75 (0.75-1.75)	0.75 (0.5-2)	**0.9**	1 (0.5-1)	0.5
CLpo (L/hr)	144 (21)	137 (60)	**140 (47)**	105 (39)	55.7	13.3 (41)	13.3 (48)	**13.3 (47)**	7.0 (25)	4.6	8.2 (43)	8.6 (44)	**8.4 (42)**	4.9 (26)	2.7
p-value#			0.13		n/a			**0.001**		n/a			**0.001**		n/a
CLsys (L/hr)	32.4 (20)	33.0 (28)	**32.8 (24)**	24.1 (17)	19.1	11.6 (33)	12.5 (43)	**12.1 (38)**	7.1 (28)	5.1	7.6 (26)	9.0 (38)	**8.4 (34)**	5.2 (27)	3.5
p-value#			**0.002**		n/a			**0.001**		n/a			**0.001**		n/a
Fpo*	0.22 (16)	0.23 (40)	**0.23 (31)**	0.26 (21)	0.36	0.99 (16)	0.94 (17)	**0.96 (16)**	1.02 (10)	1.09	0.93 (25)	1.05 (11)	**1 (18)**	1.08 (8.4)	1.33

This article is protected by copyright. All rights reserved.

Accepted Article

$t_{1/2}$ (hr)*	2.76	2.75	**2.75**	3.05	5.25	5.66	5.69	**5.68**	6.51	9.78	8.83	8.72	**8.77**	8.92	19.28
	(57)	(48)	**(49)**	(58)		(29)	(37)	**(33)**	(33)		(35)	(45)	**(40)**	(29)	
1OH/MDZ AUCR	0.53	0.40	**0.45**	0.34	0.44	0.20	0.13	**0.15**	0.09	0.08	0.12	0.11	**0.11**	0.05	0.06
	(39)	(35)	**(38)**	(22)		(32)	(49)	**(47)**	(43)		(46)	(41)	**(42)**	(29)	
p-value#			**0.038**		n/a			**0.017**		n/a			**0.00008**		n/a

Five CYP3A5 genotypes (mean±SD)*: CYP3A5*1/*1* (N=6; 4 males; BMI 25±3; age 34±14); *CYP3A5*1/*3* (N=7; 7 males; BMI 27±3; age 31±10); *CYP3A5*1/*6* (N=2); *CYP3A5*3/*3* (N=8; 6 males; BMI 25±3; age 27±8); and *CYP3A5*3/*7* (N=1). Expressers: combined *CYP3A5*1/*1*, *CYP3A5*1/*3*, and *CYP3A5*1/*6* genotype groups; Cmax, maximum blood concentration; Tmax, time of Cmax; CLpo, oral clearance; Fpo, oral bioavailability; CLsys, systemic clearance; $t_{1/2}$, terminal half-life; 1OH/MDZ AUCR, 1'-hydoxymidazolam to midazolam plasma AUC ratio after IV midazolam.Averages are geometric means (coefficient of variation * 100) except for Tmax where the median and range is presented. Comparison statistics: paired t-test of the log-transformed values, except for Tmax. *No significant difference between expressers (*CYP3A5*1/*1* and *CYP3A5*1/*x*) and non-expressers (*CYP3A5*3/*3*). #Comparison of expressers and non-expressers; n/a not included in t-test. Differences in pharmacokinetic parameters between genotypes and treatment phases were considered statically significant at the 5% level of probability with paired t-test (JMP Statistics, Version 5.0.1; SAS Institute, Cary NC).

.

This article is protected by copyright. All rights reserved.

Table 2. CYP3A abundance by CYP3A5 phenotypes in the human hepatic and small intestinal microsomal samples

CYP3A5			Human Hepatic Microsomes				Human Intestinal Microsomes		
		N	CYP3A4 (pmol/mg)	CYP3A5 (pmol/mg)	Total CYP3A (pmol/mg)	N	CYP3A4 (pmol/mg)	CYP3A5 (pmol/mg)	Total CYP3A (pmol/mg)
Predicted Phenotype	Genotype		Mean (%CV)	Mean (%CV)	Mean (%CV)		Mean (%CV)	Mean (%CV)	Mean (%CV)
CYP3A5 expressers	CYP3A5*1/*1	11	101 (69)	36.1 (84)	137 (66)	2	7.76 (10)	1.17 (43)	8.93 (3)
	CYP3A5*1/*x[#]	23	70.3 (117)	17.9 (80)	88.2 (106)	5	14.1 (70)	2.12 (79)	15.8 (60)
	All expressers	34	80.1* (98)	23.8 (92)	104 (91)	7	12.3* (70)	1.81 (78)	13.9 (61)
CYP3A5 non-expressers	CYP3A5*3/*3[&]	98	58.8* (93)	1.44 (127)	60.2 (90)	5	8.31* (74)	0.0724 (138)	8.39 (74)
Unknown	Unknown	4	52.8 (75)	1.4 (86)	54.2 (75)	NA			
Total		136	63.9 (96)	7.03 (210)	71 (97)	12	10.6 (72)	1.4 (101)	11.6 (68)

#: Two *CYP3A5*1/*6* were combined with *CYP3A5*1/*3* into one group in the human hepatic microsomal samples. One small intestinal microsomal samples with *CYP3A5*1/*3* genotype was excluded from CYP3A5 abundance data analyses as the CYP3A5 abundance was below the lower limit of quantification.

&: Five hepatic and three small intestinal microsomal samples with *CYP3A5*3/*3* genotypes were excluded from final data analyses as the CYP3A5 abundance was below the lower limit of quantification.

* $P > 0.05$, CYP3A4 abundance between CYP3A5 expressers and CYP3A5 non-expressers was not significantly different using two-tailed t-test and a P-value < 0.05 was considered significant.

This article is protected by copyright. All rights reserved.

Table 3. Observed and simulated oral and systemic blood clearance values following a single dose of midazolam in healthy CYP3A5 expressers and non-expressers

		Clearance (L/hr)		CL ratio of Exp to Non-exp	
		IV	Oral	IV	Oral
		GM (90% CI)	GM (90% CI)		
Observed	CYP3A5 non-expressers	24.1 (21.7-26.7)	105 (83.5-131.5)	1.4	1.3
	CYP3A5 expressers	32.8 (29.5-36.3)	140 (114.5-171.3)		
Scenario 1	Simcyp default				
	CYP3A5 non-expressers	36.7 (34.8-38.6)	125.8 (115.0-137.7)	1.5	3.3
	CYP3A5 expressers	56.8 (55.1-58.6)	413.5 (382.1-447.5)		
Scenario 2	Modified hepatic CYP3A abundance with measured CV + Simcyp intestinal CYP3A				
	CYP3A5 non-expressers	22.6 (20.5- 24.8)	62.8 (54.9-71.9)	1.4	2.0
	CYP3A5 expressers	31.2 (29.1-33.5)	128.0 (113.9-143.8)		
Scenario 3	Modified hepatic CYP3A abundance with 50% of measured CV+ Simcyp intestinal CYP3A				
	CYP3A5 non-expressers	25.9 (24.3-27.7)	72.9 (66.3-80.1)	1.3	2.0
	CYP3A5 expressers	34.4 (32.7-36.3)	144.1 (132.1-157.2)		
Scenario 4	Modified hepatic CYP3A abundance with 33% of measured CV+ Simcyp intestinal CYP3A				
	CYP3A5 non-expressers	26.9 (25.5-28.3)	75.7 (70.0-82.1)	1.3	2.0
	CYP3A5 expressers	35.3 (33.8-36.9)	148.1 (137.2-160.0)		
Scenario 5	Modified hepatic CYP3A abundance with 33% of measured CV+ modified intestinal CYP3A				
	CYP3A5 non-expressers	27.1 (25.8-28.6)	104.2 (95.4-113.9)	1.3	1.8
	CYP3A5 expressers	35.6 (33.8-37.1)	185.3 (168.2-200.9)		

CV: coefficient of variation; GM: geometric mean; SD: standard deviation; CL: clearance

Simulation scenarios: 1) SimCYP values for hepatic and small intestinal CYP3A abundance and variability; 2-4) LC/MS-measured hepatic CYP3A abundance with adjusted variability plus SimCYP small intestinal CYP3A abundance and variability; and 5) LC/MS-measured hepatic CYP3A abundance with optimized variability plus optimized small intestinal CYP3A abundance

Correlation for the modified hepatic CYP3A4 and CYP3A5 abundance in CYP3A5 expressers is described as (in pmol/mg) CYP3A5 = 0.18*CYP3A4 + 9.55. Simulations were conducted in total 100 healthy subjects including 10 trial with 10 healthy subjects in each trial

Accepted Article

This article is protected by copyright. All rights reserved.

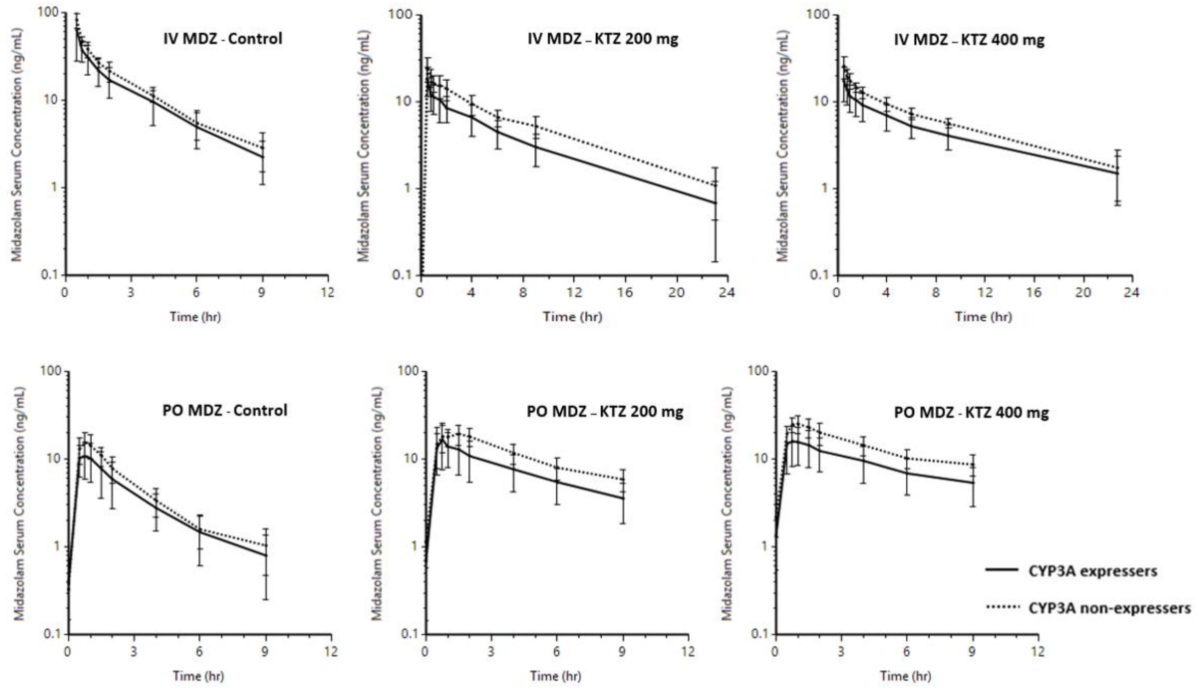

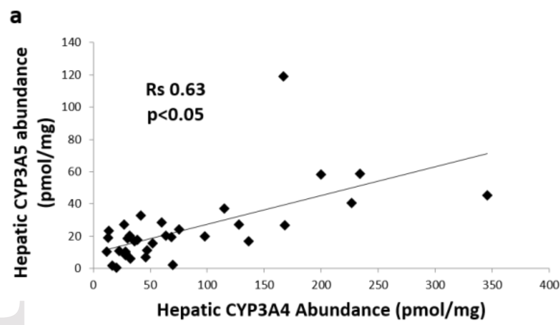

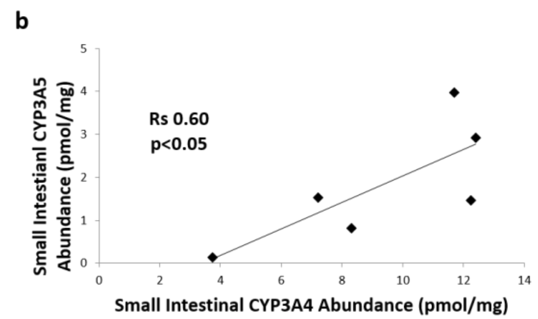

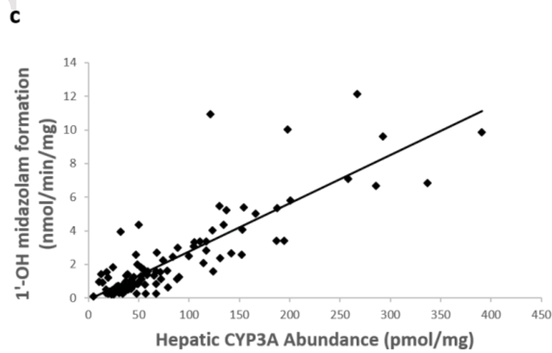

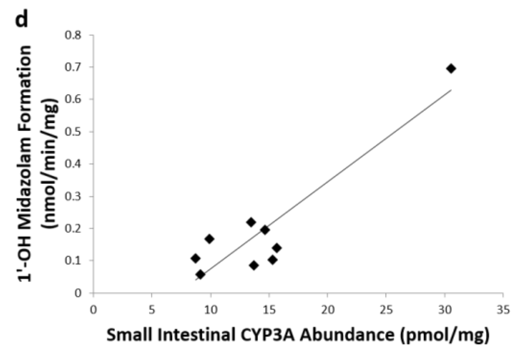

This article is protected by copyright. All rights reserved.

Accepted Article

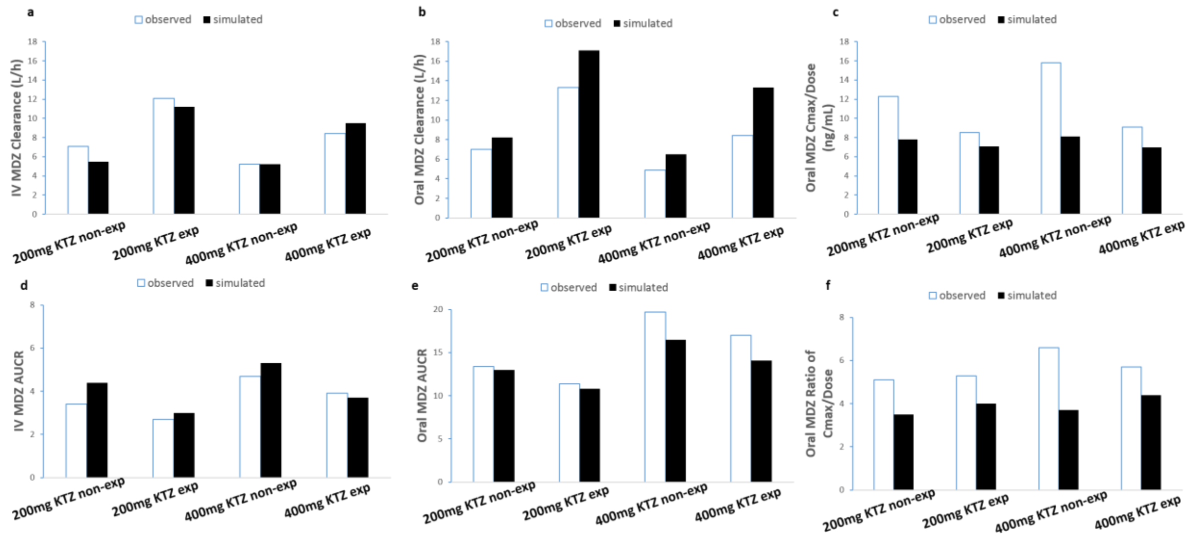

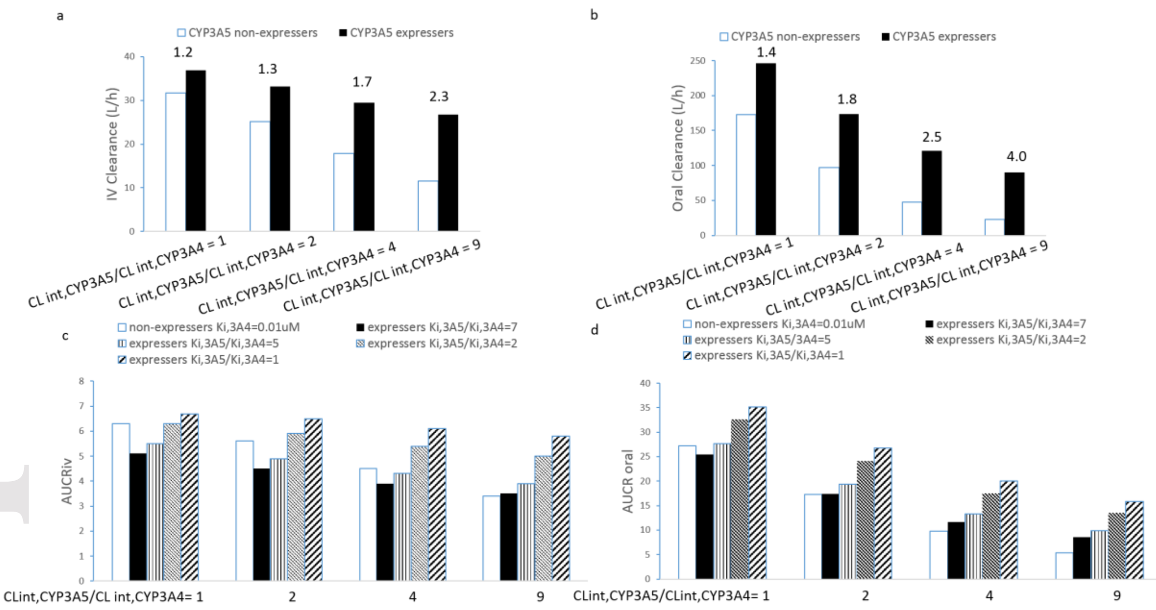

This article is protected by copyright. All rights reserved.